Supplemental material

Idikuda et al., **https://doi.org/10.1085/jgp.201711961**

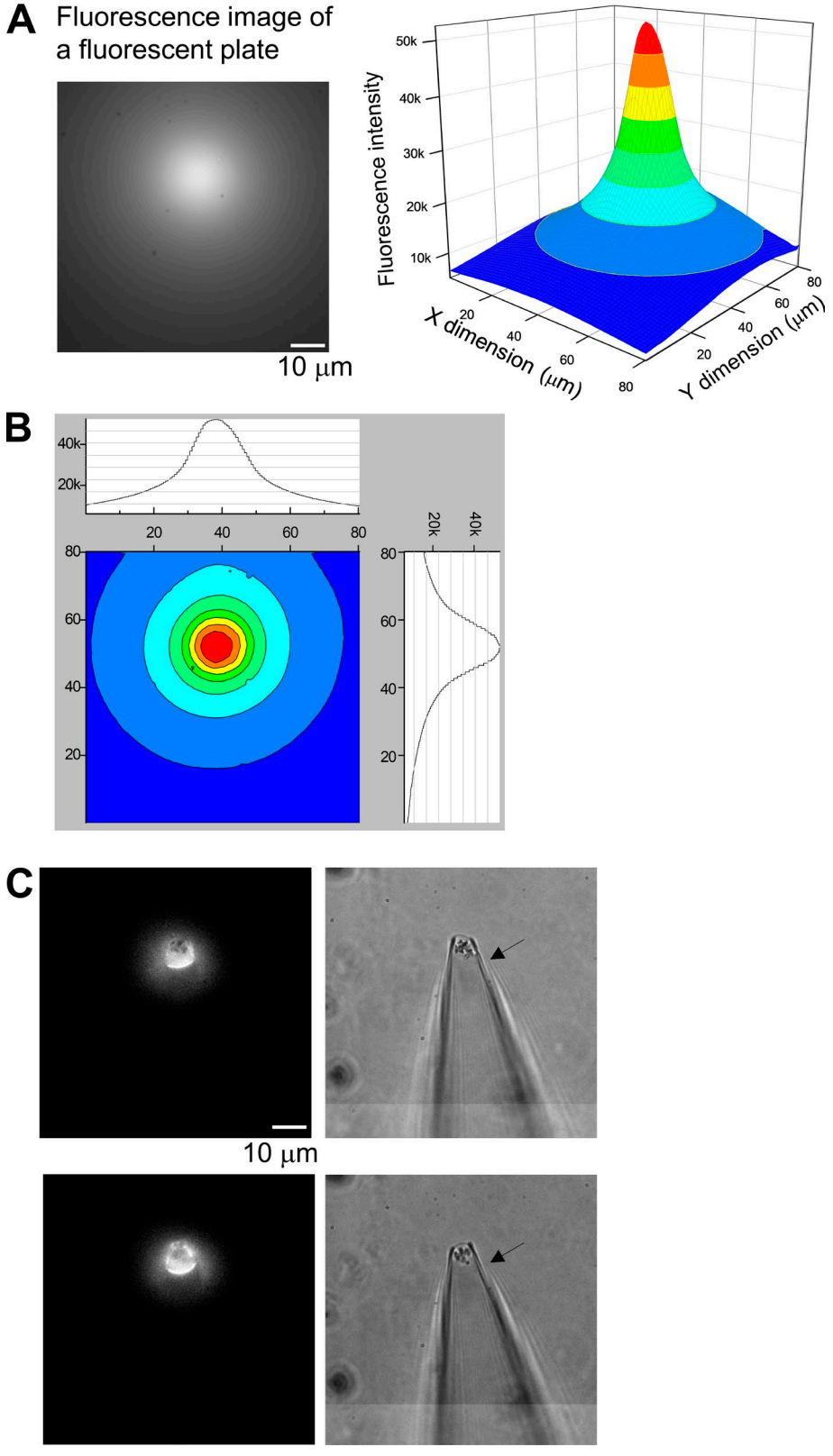

Figure S1. **Intensity profile of the excitation light and alignment of membrane patches. (A)** A fluorescent plate (Chroma Technology Corp.) was mounted at the focal plane of the objective lens. Left: A fluorescence image was collected by the same optical configuration (473-nm laser, filter sets and dichroic mirror, EMCCD camera) as for membrane patches. The exposure time and gain of the camera were reduced to prevent saturation (65,535 for a 16-bit camera). Right: Color map surface illustration of the distribution of fluorescence intensity. **(B)** A color contour map of the fluorescence intensity is shown in the center. Top and right: projections to X and Y dimension, respectively, from the peak of the intensity. **(C)** Fluorescence (left) and bright-field (right) images of two membrane patches. 1 μM FITC-cAMP was added to the bath solution. Arrows indicate the position of the membrane patch.

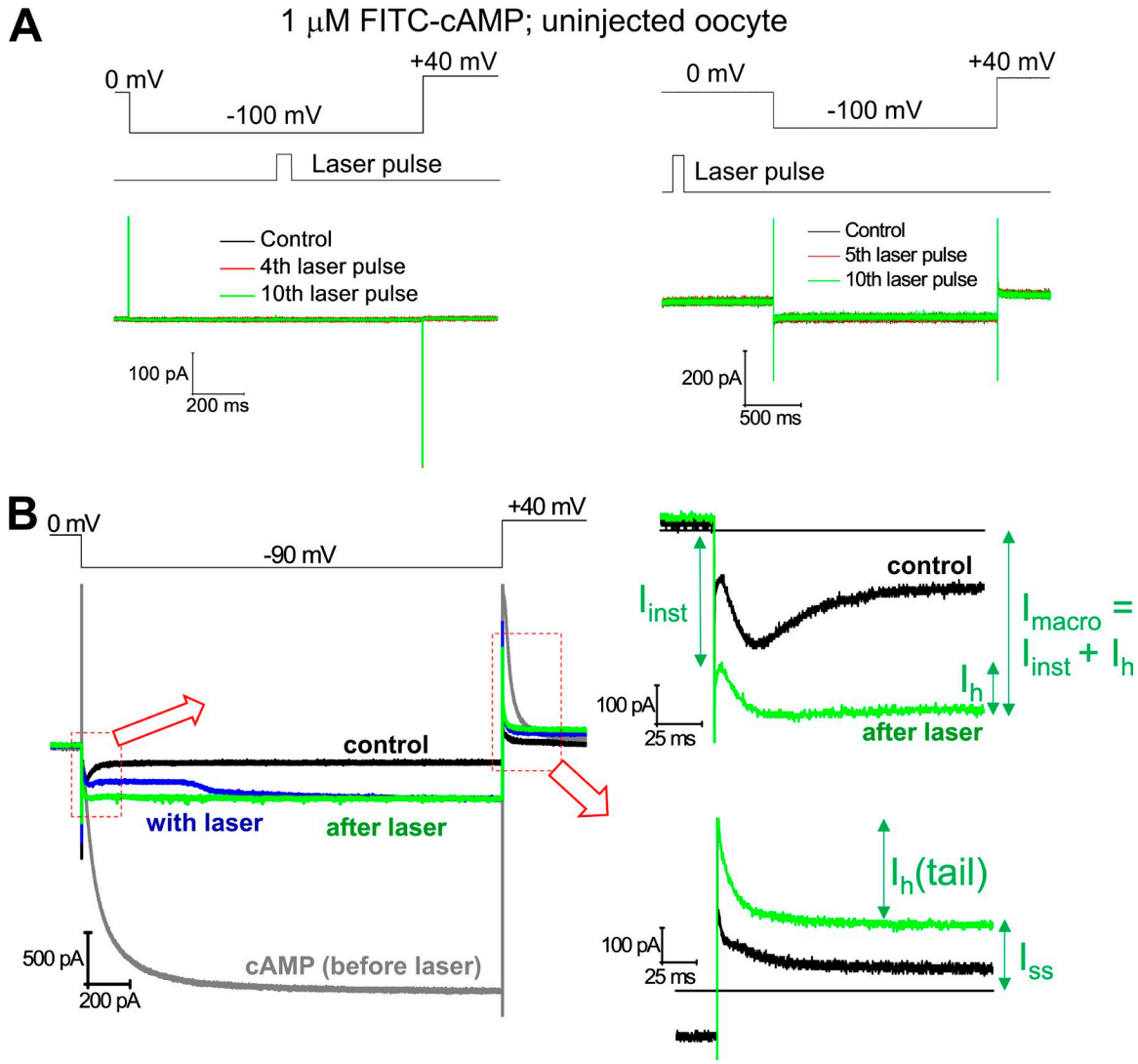

Figure S2. **Effects of photodynamic modification on cell membrane without spHCN channel and illustration of I_{inst}, I_h, I_h (tail), and I_{ss} after photodynamic modification. (A)** Top: Voltage command and timing of laser pulse (during voltage step). Bottom: Current traces recorded from uninjected oocytes before and after laser pulse application. Black, last control current trace before laser pulses. Green, current traces in response to laser pulses. Left: Laser pulse during voltage step. Right: Laser pulse before voltage step. **(B)** Left: Current traces recording in sequence control (black), with cAMP (gray), with laser (blue), after end of laser pulse (green). Also see Fig. 2 A. Right: Labeling of I_{inst}, I_h, I_h(tail), and I_{ss} for the current trace after end of laser pulse (green).

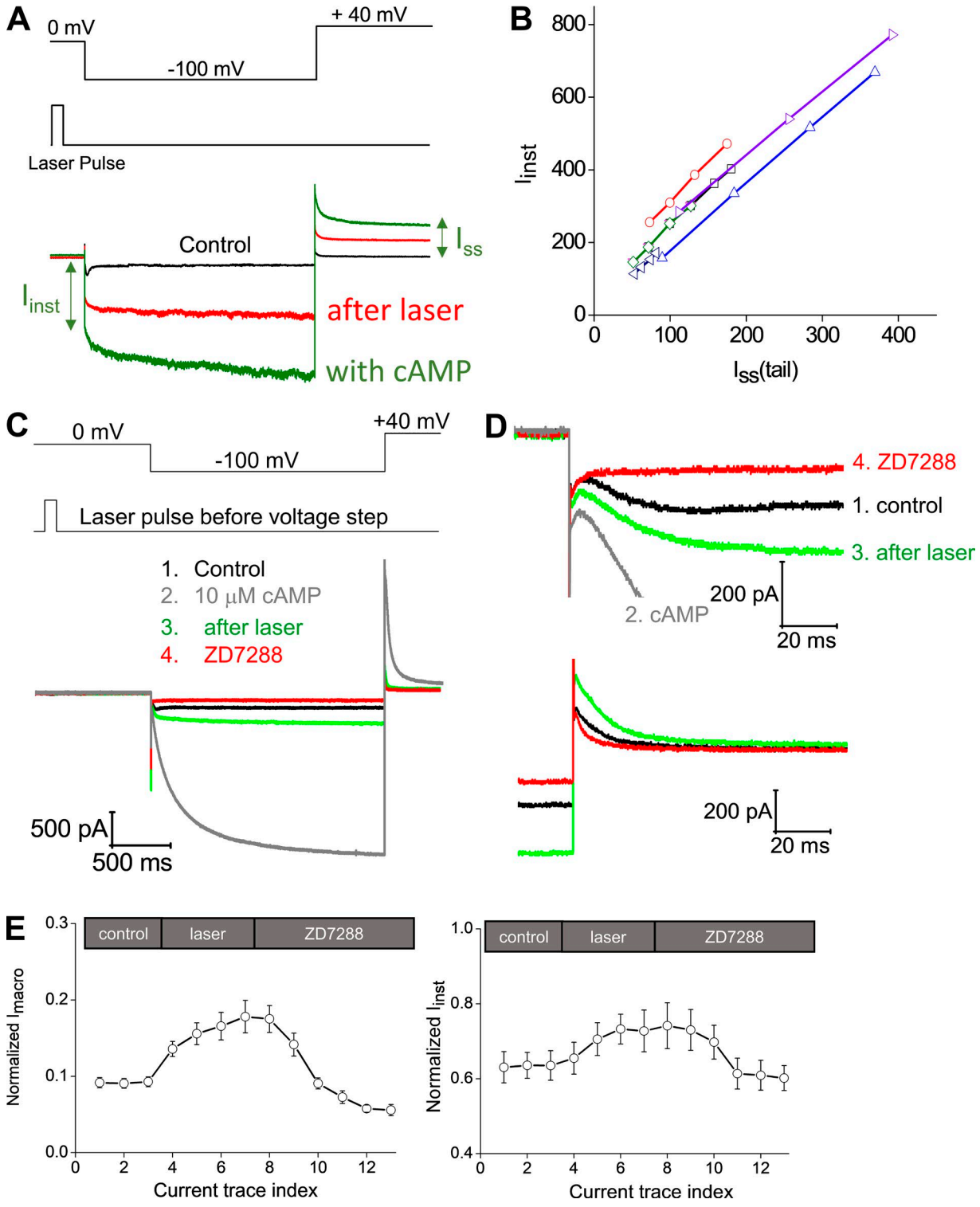

Figure S3. **I_{inst} and I_{ss} after photodynamic modification can be up-regulated by cAMP and blocked by ZD7288. (A)** Top: Protocol of voltage step and laser pulse. Bottom: Current traces before laser pulses (control; black), 5 min after laser pulse stopped and FITC-cAMP washed off (red), and 10 μM cAMP (green). **(B)** Cross-plotting the amplitudes of I_{inst} and I_{ss} of WT spHCN channel after photodynamic modification. Four sequential laser pulses were applied in the middle of the voltage step. Each point shows amplitudes of the I_{ss} of the present current trace (measured after laser pulse at +40 mV) and the I_{inst} of the following current trace (measured before the next laser pulse at −100 mV). Each set of data points represents results from a single patch. Different symbols represent different patches. **(C)** Top: Protocol of voltage step and laser pulse (before voltage step). Bottom: Four current traces in sequence showing control (no cAMP; black), regular cAMP (10 μM; gray), after laser pulses stopped and washing off FITC-cAMP (green), and ZD7288 (100 μM; red). **(D)** Zoomed view showing the I_{inst} (top) or the I_h(tail) and I_{ss} (bottom). **(E)** Averaged results of I_{macro} (left) and I_{inst} (right) in response to laser pulses (before voltage step) and ZD7288.

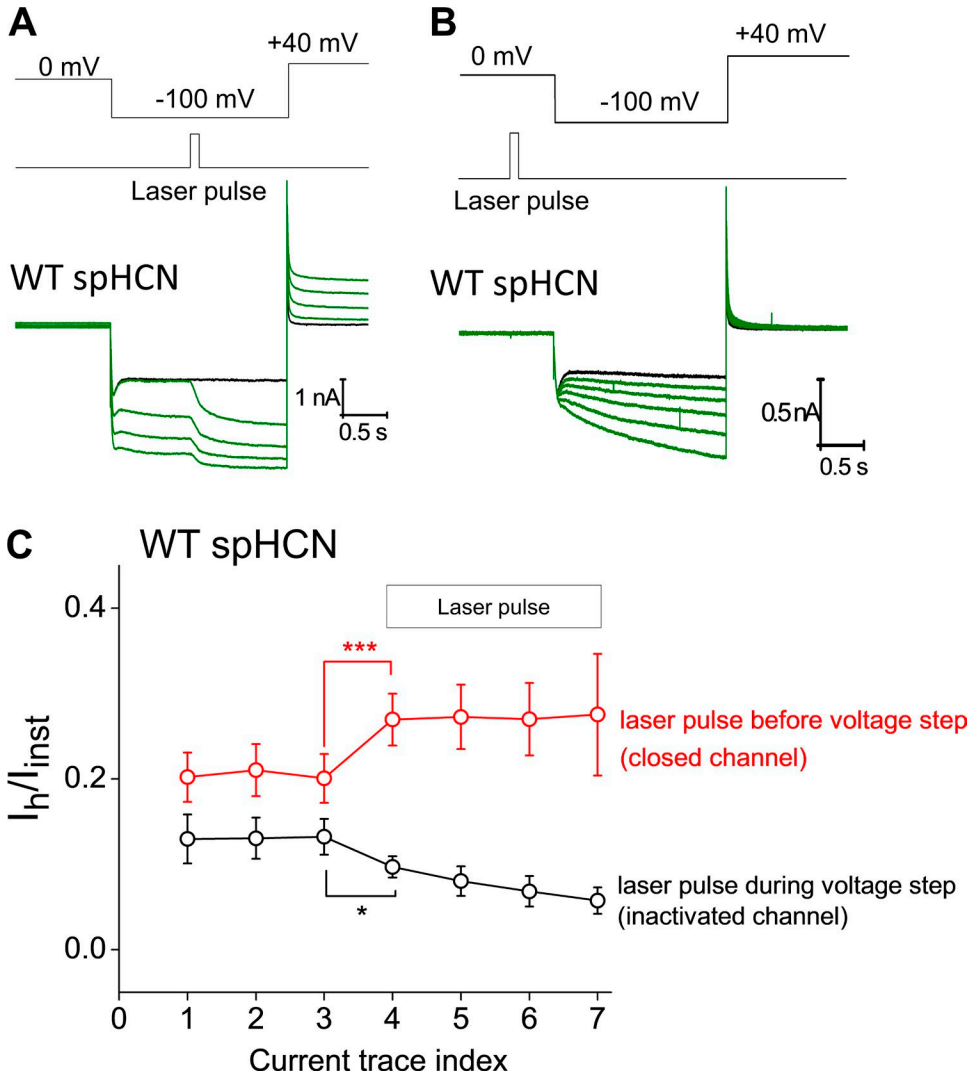

Figure S4. **Laser pulses applied before and in the middle of the hyperpolarizing voltage step have different impact on I_{inst} and I_h(tail). (A)** Top: Voltage command and timing of laser pulse (during voltage step). Bottom: Current traces before and after laser pulses. Black, current trace before the first laser pulse. Green, current traces in response to laser pulses. **(B)** Top: Voltage command and timing of laser pulse (during voltage step). Bottom: Current traces before and after laser pulses. Black, current trace before the first laser pulse. Green, current traces in response to laser pulses. **(C)** Ratio of I_h/I_{inst} plotted as a function of current trace index. Laser pulses started from the fourth episode. Red, laser pulse before voltage step (n = 16). Black, laser pulse after laser pulse (n = 10). Mean ± SEM; *, P ≤ 0.05; ***, P ≤ 0.001.

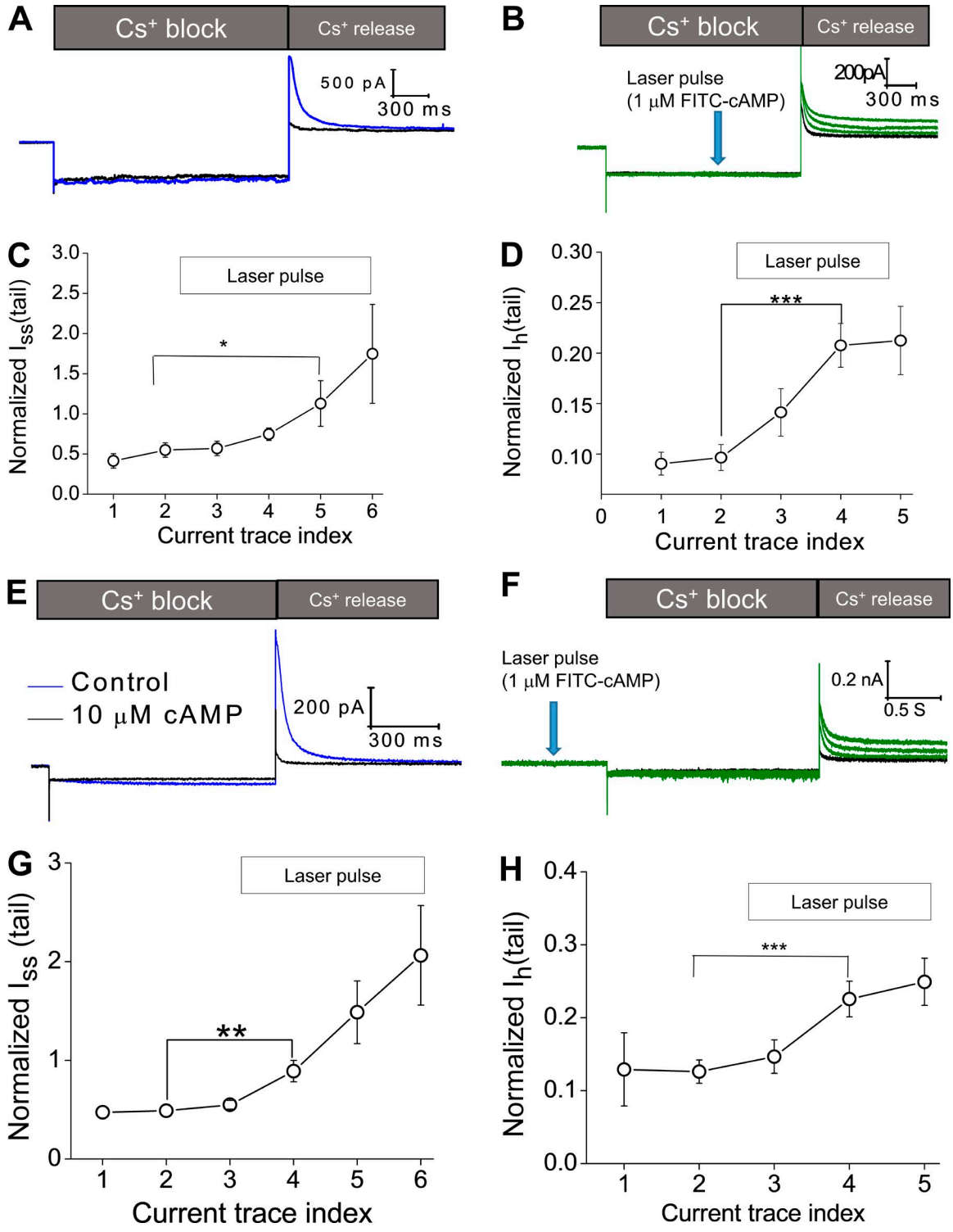

Figure S5. **Cs⁺ blocks I_{inst} and I_h after photodynamic modification. (A)** WT spHCN current traces recorded before laser pulses. Black, control; blue, 10 μM cAMP. 2 mM Cs⁺ applied to the glass pipette or the extracellular side of the membrane blocks spHCN currents at −100 mV. The block by Cs⁺ can be released by a depolarizing voltage step from −100 to +40 mV. **(B)** Current traces showing the effect of laser pulse (during voltage step) on the WT spHCN channel in the presence of Cs⁺. Black, last control current trace before the first laser pulse. Green, current traces in response to laser pulses. **(C)** Averaged results showing the effect of laser pulses (during voltage step) on I_{ss}(tail; n = 6). *, P ≤ 0.05. **(D)** Averaged results showing the effect of laser pulses (during voltage step) on I_h(tail; n = 5). ***, P ≤ 0.001. **(E)** Current traces recorded with 2 mM Cs⁺ added to the pipette solution. Black, control; blue, 10 μM cAMP. **(F)** Current traces recorded in the presence of 1 μM FITC-cAMP and the responses to laser pulse (before voltage step). Black, last control current trace before the first laser pulse. Green, current traces in response to laser pulses. **(G)** Averaged results showing the effect of laser pulses (before voltage step) on the I_{ss}(tail; n = 7). **, P ≤ 0.01. **(H)** Averaged results (n = 8) showing the effect of laser pulses (before voltage step) on I_h(tail). ***, P ≤ 0.001.

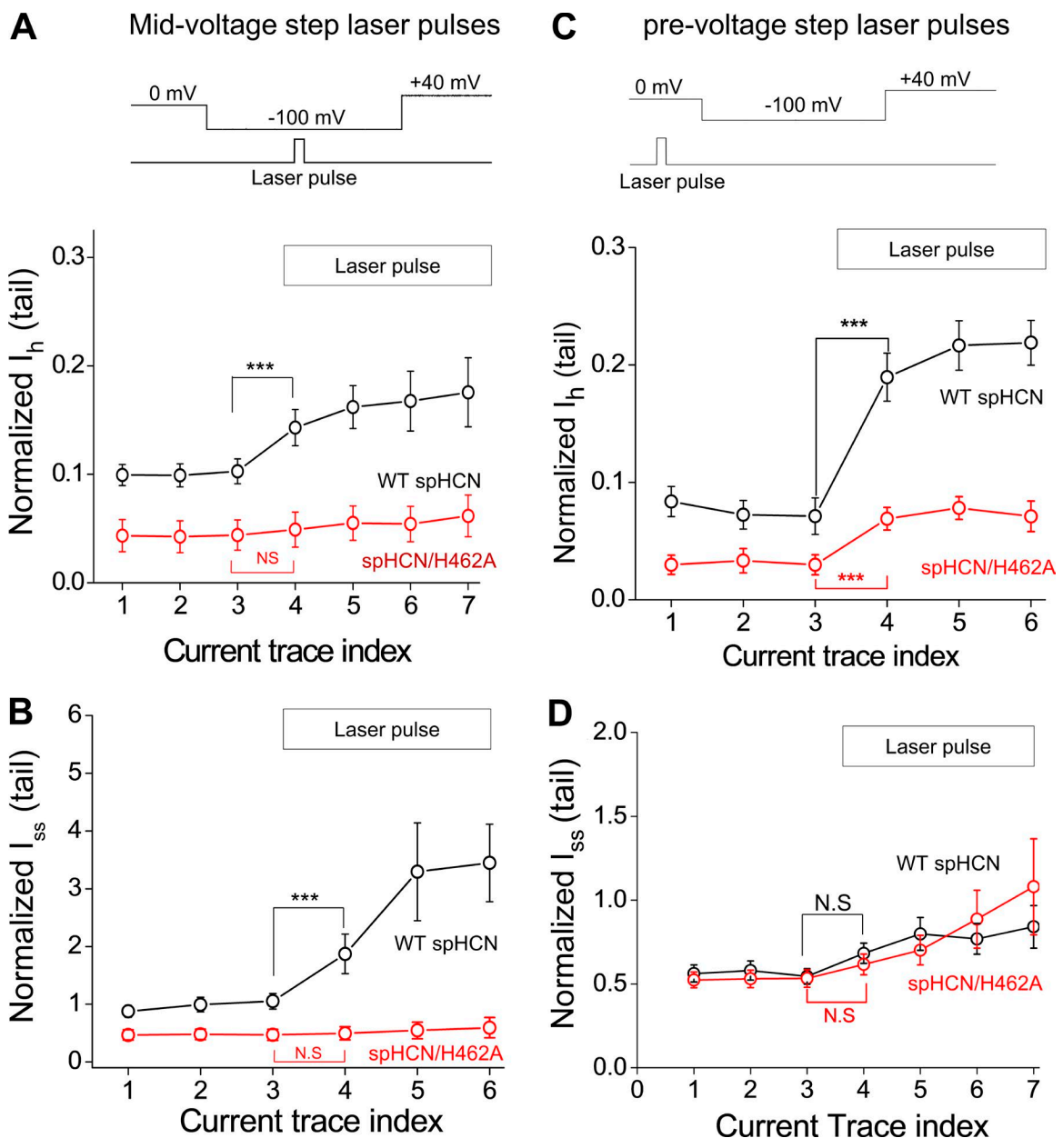

Figure S6. **WT spHCN channel is more sensitive to photodynamic modification than spHCN/H462A mutant channel. (A)** Averaged results showing the effect of laser pulses (during voltage step) on the I_h(tail) of the WT (n = 13; black) and spHCN/H462A mutant (n = 4; red) channels. ***, P ≤ 0.001. **(B)** Averaged results showing the effect of laser pulses (during voltage step) on the I_{ss}(tail) of the WT (n = 13; black) and spHCN/H462A mutant (n = 5; red) channels. ***, P ≤ 0.001. **(C)** Averaged results showing the effect of laser pulses (before voltage step) on the I_h(tail) of the WT (n = 15; black) and spHCN/H462A mutant (n = 4; red) channels. ***, P ≤ 0.001. **(D)** Averaged results showing the effect of laser pulses (before voltage step) on the I_{ss}(tail) of the WT (n = 15; black) and spHCN/H462A mutant (n = 5; red) channels.

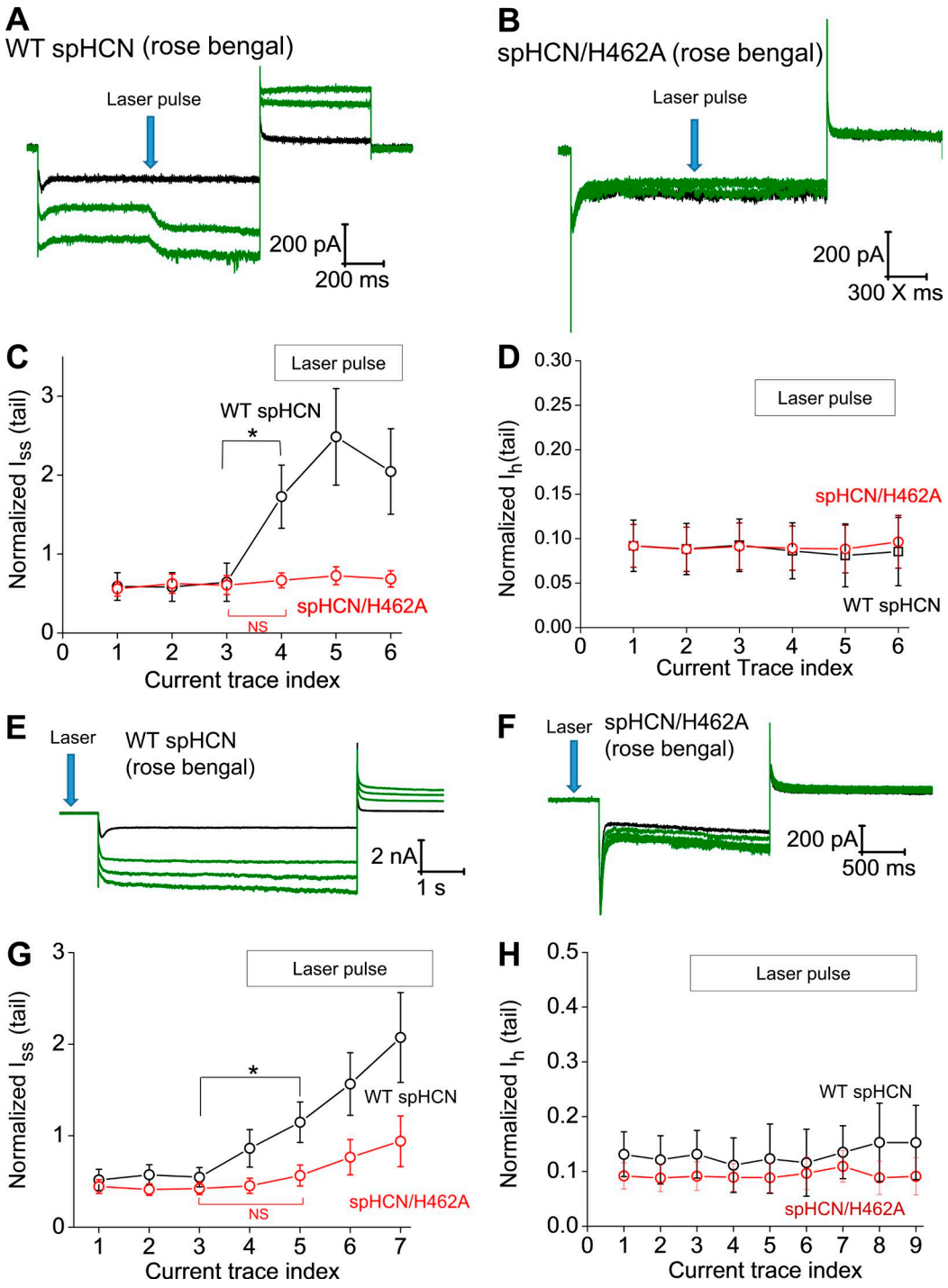

Figure S7. **Rose Bengal–mediated photodynamic modification of WT spHCN and spHCN/H472A mutant channels. (A)** Representative current traces showing the effect of laser pulses (during voltage step) on the WT spHCN channel in the presence of 100 nM Rose Bengal. Black, last control current trace before the first laser pulse. Green, current traces with laser pulses. **(B)** Representative current traces showing the effect of laser pulses (during voltage step) on the spHCN/H462A channel in the presence of 100 nM Rose Bengal. Black, last control current trace before the first laser pulse. Green, current traces in response to laser pulses. **(C)** Averaged results showing the effect of laser pulses (during voltage step) on the I_{ss}(tail) of the WT (n = 6, black) and spHCN/H462A mutant (n = 7, red) channels. *, P ≤ 0.05. **(D)** Averaged results showing the effect of laser pulses (during voltage step) on the I_h current of the WT (n = 6, black) and spHCN/H462A mutant (n = 8, red) channels. **(E)** Representative current traces showing the effect of photodynamic modification on the WT spHCN channel (before voltage step) in the presence of 100 nM Rose Bengal. Black, last control current trace before the first laser pulse. Green, current traces in response to laser pulses. **(F)** Representative current trace showing the effect of photodynamic modification on spHCN/H462A channel (before voltage step) in the presence of 100 nM Rose Bengal. Black, last control current trace before the first laser pulse. Green, current traces in response to laser pulses. **(G)** Averaged results showing the effect of laser pulses (before voltage step) on the I_{ss}(tail) of the WT (n = 7, black) and spHCN/H462A mutant (n = 5, red) channels. *, P ≤ 0.05. **(H)** Averaged results showing the effect of laser pulses (before voltage step) on the I_h of the WT (n = 5, black) and spHCN/H462A mutant (n = 5, red) channels.

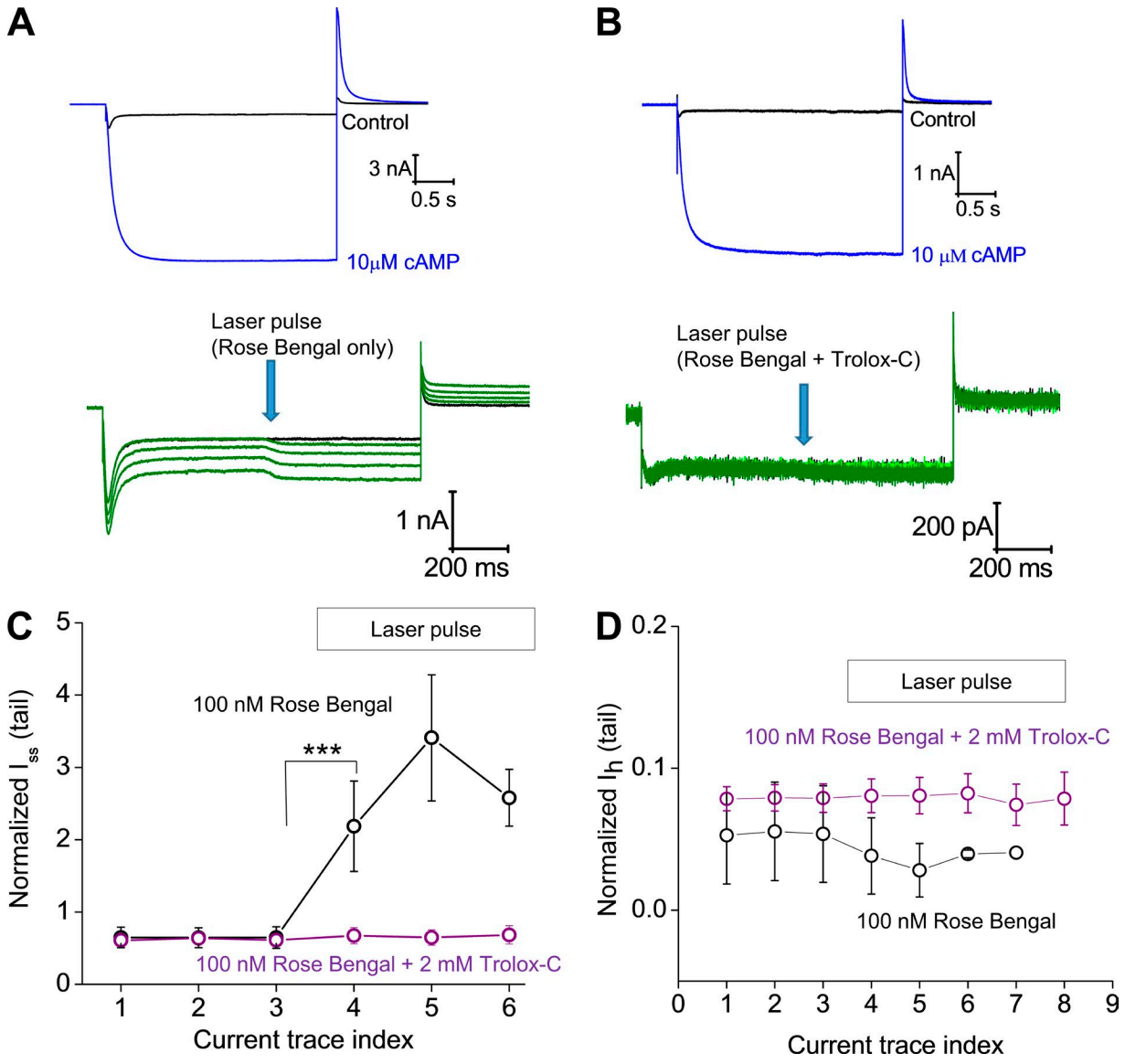

Figure S8. **Effects of singlet oxygen quencher Trolox-C on the photodynamic modification of inactivated spHCN channels mediated by Rose Bengal. (A)** Top: Current traces of the WT spHCN channel before (black) and after (blue) adding 10 μM cAMP. Bottom: Responses of the WT spHCN channel to laser pulses (during voltage step) in the presence of 100 nM Rose Bengal (green). **(B)** Top: Current trace recorded from the WT spHCN channel before (black) and after (blue) adding 10 μM cAMP. Bottom: Responses of WT spHCN channel to laser pulses (during voltage step) in the presence of Rose Bengal and 2 mM Trolox-C (green). **(C)** Averaged results showing the effect of laser pulses on I_{ss}(tail) without (n = 11, black) or with (n = 6, purple) 2 mM Trolox-C. ***, P ≤ 0.001. **(D)** Averaged results showing the effect of laser pulses on I_h(tail) without (n = 11, black) or with (n = 6, purple) 2 mM Trolox-C.

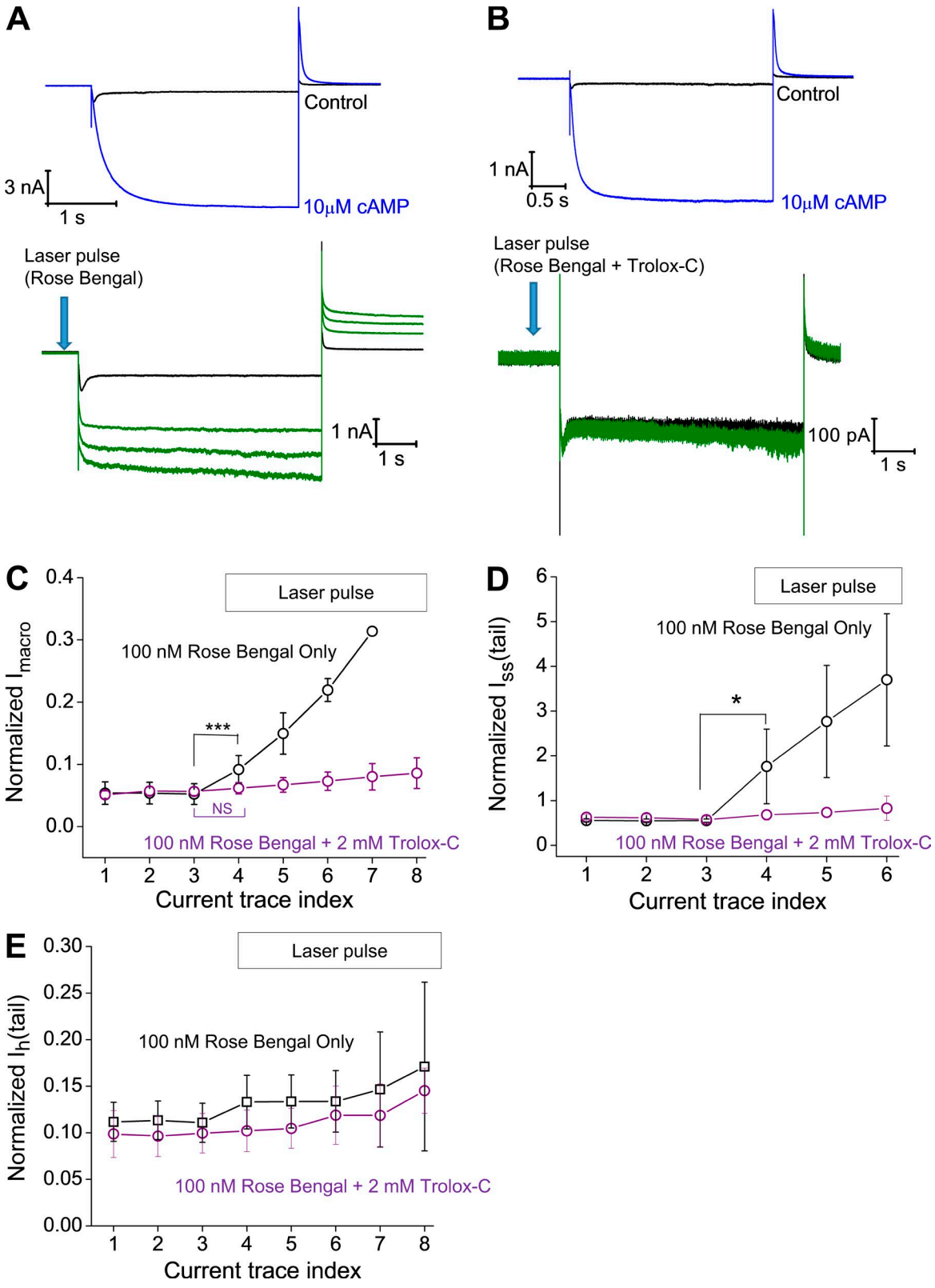

Figure S9. **Effects of Trolox-C on the photodynamic modification of closed spHCN channels mediated by Rose Bengal. (A)** Top: Current traces of the WT spHCN channel before (black) and after (blue) adding 10 μM cAMP. Bottom: Responses of the WT spHCN channel to laser pulses (before voltage step) in the presence of 100 nM Rose Bengal (green). **(B)** Top: Current traces recorded from the WT spHCN channel before (black) and after (blue) adding 10 μM cAMP. Bottom: Responses of the WT spHCN channel to laser pulses (before voltage step) in the presence of Rose Bengal and 2 mM Trolox-C (green). **(C)** Averaged results showing the effect of laser pulses on I_{macro} without (n = 9, black) and with (n = 6, purple) 2 mM Trolox-C. ***, P ≤ 0.001. **(D)** Averaged results showing the effect of laser pulses on I_{ss}(tail) without (n = 9, black) and with (n = 6, purple) 2 mM Trolox-C. *, P ≤ 0.05. **(E)** Averaged results showing the effect of laser pulses on I_h(tail) without (n = 9, black) and with (n = 6, purple) 2 mM Trolox-C.

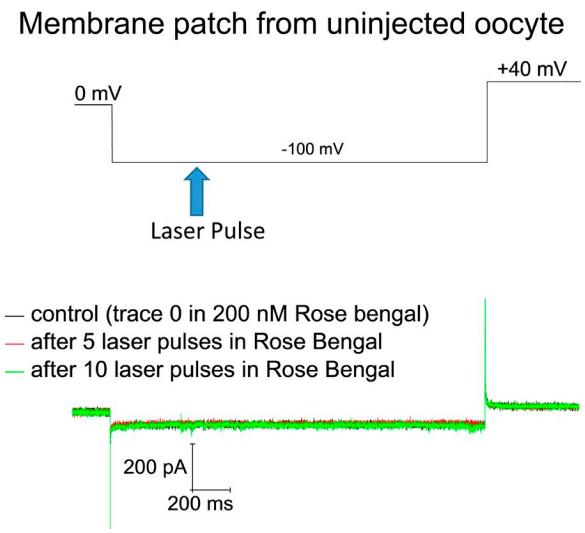

Figure S10. **Rose Bengal with laser pulses has no effects on empty membrane patch without spHCN channel.** Top: Protocol of voltage and laser pulse (during voltage step). 100-ms laser pulse duration. Bottom: Leak currents recorded from membrane patches pulled from uninjected *Xenopus* oocyte. Rose Bengal (200 nM) was applied to the bath solution. Black, control trace before laser pulse. Red, current trace with the fifth laser pulse. Green, current trace with the 10th laser pulse.

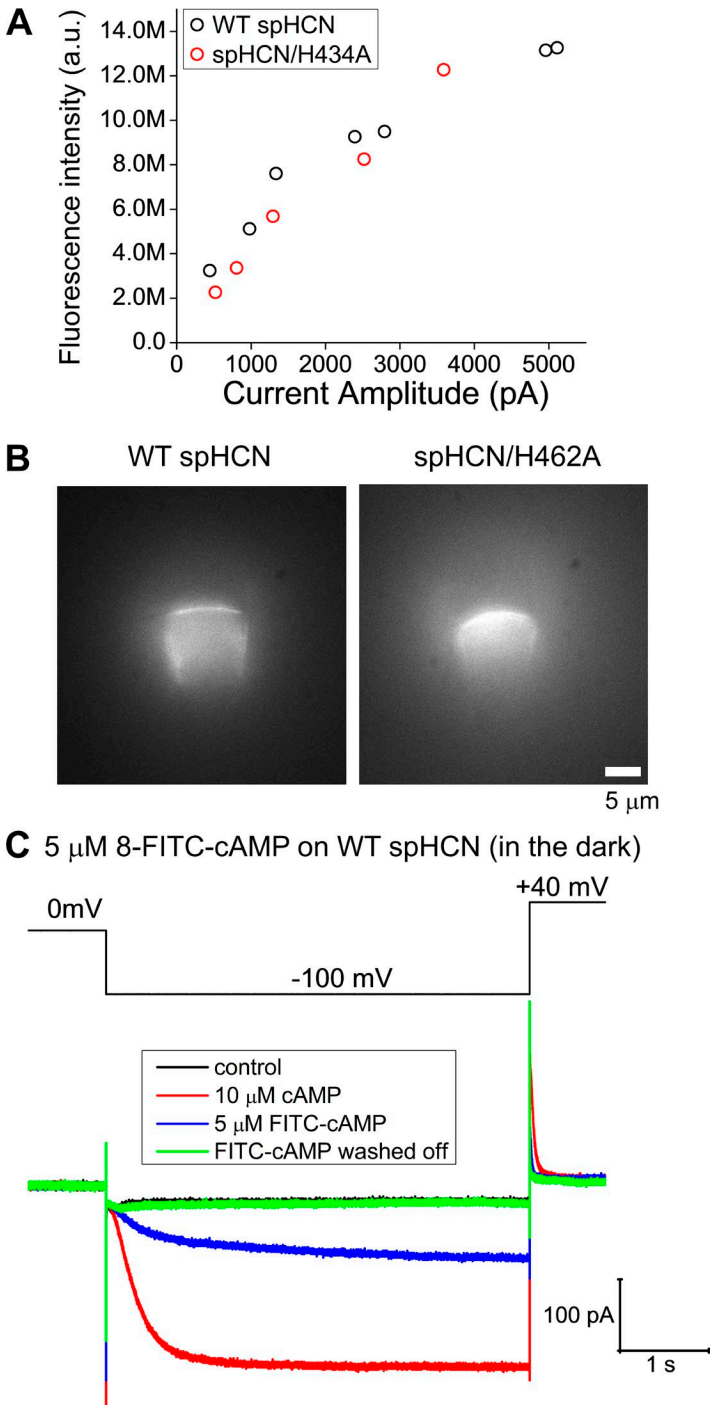

Figure S11. **WT spHCN and spHCN/H462A mutant channels show comparable binding of FITC-cAMP. (A)** Top: Current amplitude versus fluorescence intensity of WT spHCN (black) and spHCN/462A (red) channel in complex with FITC-cAMP. **(B)** Fluorescence images of WT spHCN (left) and spHCN/H462A channel (right) in the presence of 1 μM FITC-cAMP. **(C)** Effects of 5 μM FITC-cAMP on the gating of WT spHCN channel. FITC-cAMP was added in the dark to prevent any unnecessary photodynamic modifications. The order of current trace recorded: control before cAMP (black), 10 μM cAMP (red), 5 μM FITC-cAMP (blue), and FITC-cAMP washed off (magenta). After washing off 10 μM cAMP, current traces were confirmed to return to control level before adding FITC-cAMP.

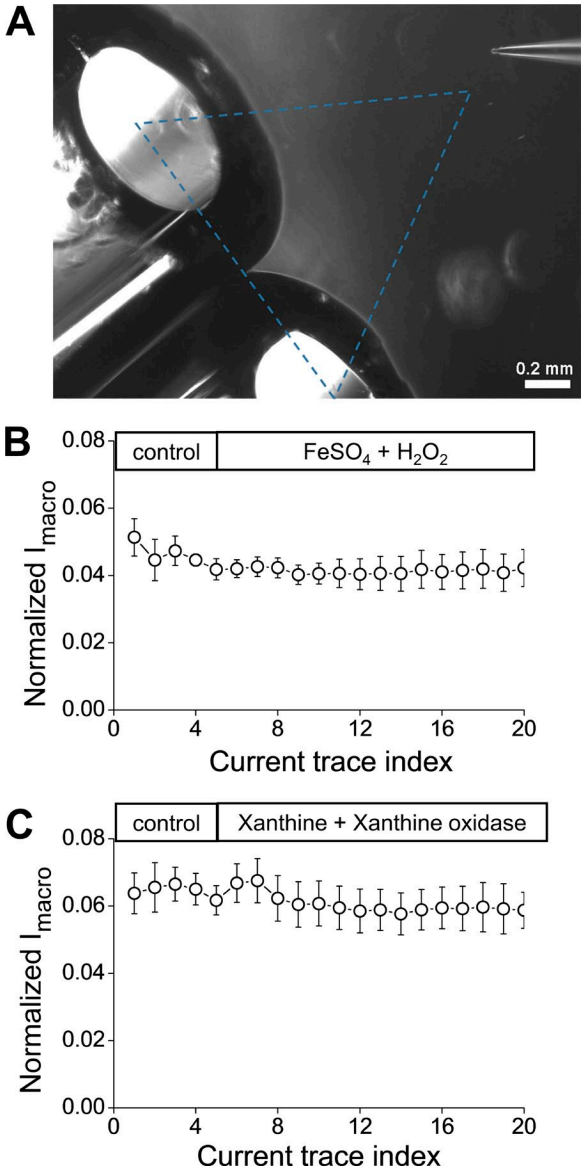

Figure S12. **Configuration of the perfusion system for H_2O_2 and ClO^- and mean results for effects of hydroxyl and superoxide radicals. (A)** Top: Configuration of the perfusion system and positioning of the recording pipette. A double-barrel glass pipette was used to deliver H_2O_2 and ClO^- in each of its tubes to the membrane patch. The X-Y position of membrane patch was adjusted according to the picture. The membrane patch was lowered to the same focal plane of the lower edge of the double-barrel pipette. **(B)** Averaged results showing the effect of 1 mM $FeSO_4$ + 15 mM H_2O_2 on I_{macro}. **(C)** Averaged results showing the effect of 5 mM xanthine + 15 mU xanthine oxidase on I_{macro}.

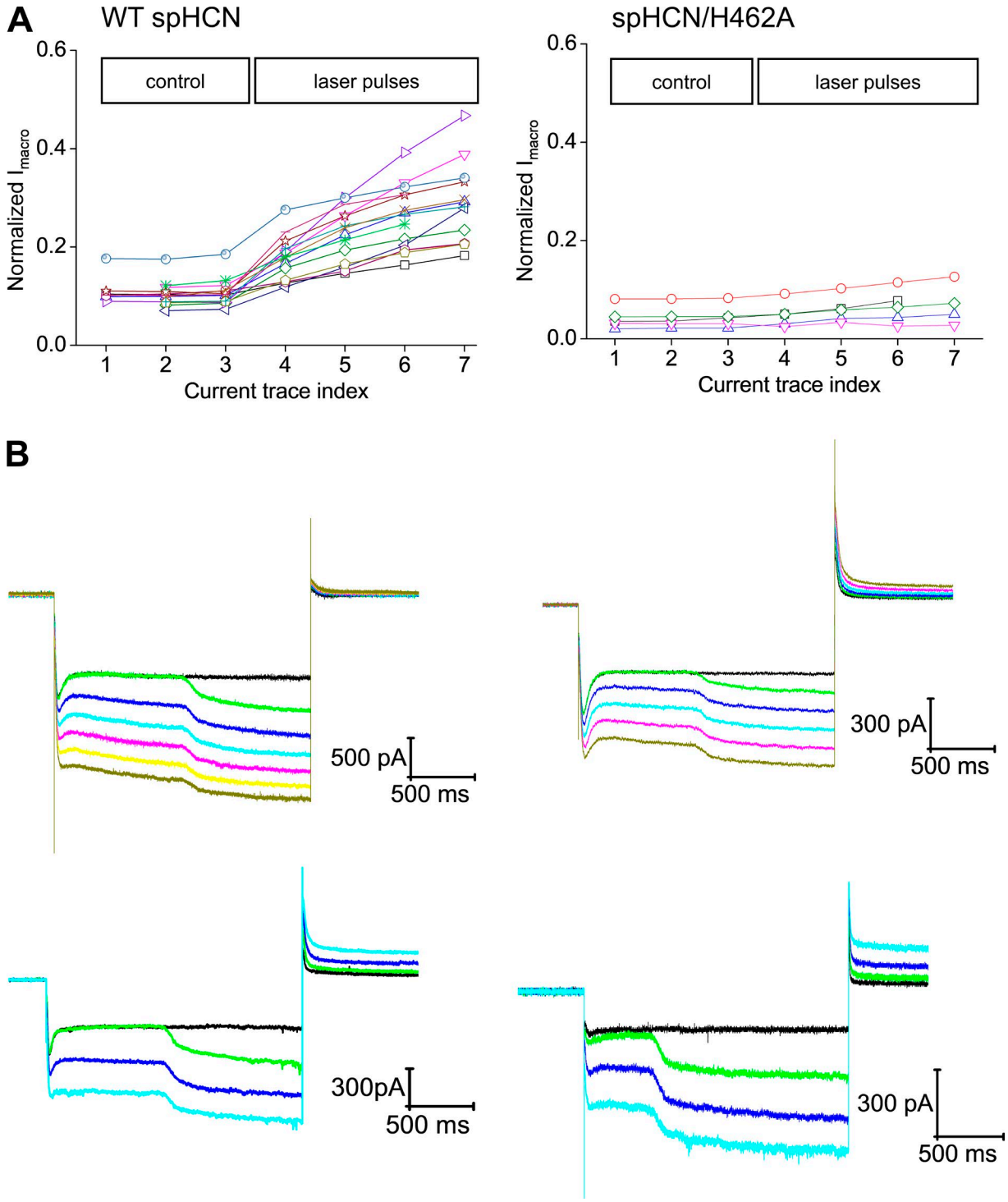

Figure S13. **Raw data for the effects of laser pulses during voltage step on amplitudes of I_{macro}. (A)** Amplitudes of I_{macro} normalized to the maximal current, which was measured before laser pulse and with 10 µM cAMP. Left, WT spHCN (laser pulse during voltage step). Right, spHCN/H462A (laser pulse before voltage step). **(B)** Representative current traces of WT spHCN channel in response to laser pulses applied during the hyperpolarization voltage step. The last trace without laser pulse is shown in black. Following traces with laser pulses are shown in color.

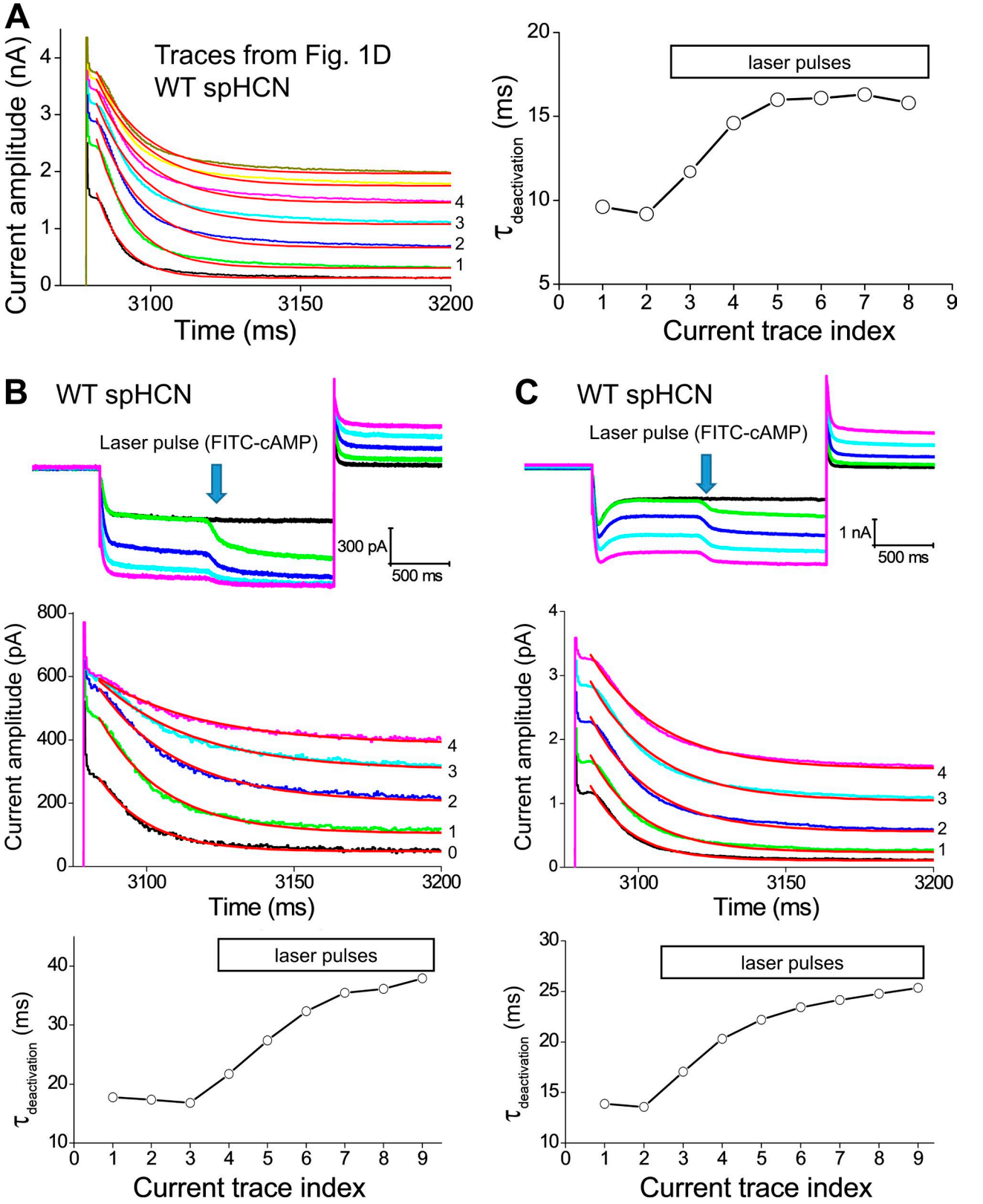

Figure S14. **Examples of single exponential fitting of deactivating tail current. (A)** Left, a zoomed view over the tail current of the traces shown in Fig. 1 D. Number left to the traces represent the order of laser pulses applied. Black, the last control trace before laser application. Thin red lines represent curve fit result. Right, time constant of tail current deactivation plotted against current trace index. **(B)** Top: Another set of current traces before (black) and after laser pulses. Middle: A zoomed view over the tail current. Thin red line represents the corresponding single exponential fits. Bottom: Time constant of tail current deactivation versus current trace index. **(C)** Results from another patch.